CrystEngComm

Accepted Manuscript

ROYAL SOCIETY OF CHEMISTRY

www.rsc.org/crystengcomm

Journal Name

RSCPublishing

ARTICLE

Synthesis and characteristics of $ZnGa_2O_4$ hollow nanostructures via carbon@$Ga(OH)CO_3$@$Zn(OH)_2$ by hydrothermal method

Cite this: DOI: 10.1039/xoxxoooooox

Received ooth January 2012,
Accepted ooth January 2012

DOI: 10.1039/xoxxoooooox

www.rsc.org/

Bong Kyun Kang,[a] Hyeong Dae Lim,[a] Sung Ryul Mang,[b] Keun Man Song,[a] Mong Kwon Jung,[c] and Dae Ho Yoon[a,b*]

$ZnGa_2O_4$ hollow nanostructures were synthesized by two steps hydrothermal and calcination processes using carbon spheres as template. We observed the carbon@$Ga(OH)CO_3$ core-shell nanostructures were covered by uniform shell of $Zn(OH)_2$ nanoparticles at 2.5 mmol of ZnAc and $ZnGa_2O_4$ hollow nanostructures with diameters of approximately 200 nm and shell thickness of around 15 nm. After calcination, the amorphous core-shell-shell nanostructures yielded highly crystalline $ZnGa_2O_4$ (ZnAc: 2.5 mmol) hollow nanostructures at 900 °C for 1 h. The shell possesses the single-crystal structure and the lattice spacing of around 0.253 nm corresponds to the d spacing of (311) crystal planes of cubic $ZnGa_2O_4$. The presence of the composition and surface electron state of $ZnGa_2O_4$ hollow nanostructures at 900 °C is confirmed by the x-ray photoelectron spectroscopy. The UV and blue emission of $ZnGa_2O_4$ hollow nanostructures were found to self-activation center octahedral sites Ga-O group in the spinel structures and distorted symmetry of octahedral sites by oxygen vacancies, respectively.

Introduction

In recent years, metal-oxide semiconductor nanomaterials such as nanotubes, wires, particles and hollow nanostructures (NSs) are attractive candidates as active elements for advanced nanoscale devices due to their unique electronic and optical properties, high specific surface area, and shell permeability that can be of importance to many areas of technology.[1-4] However, the nanomaterials have to involve some breakthrough to improve their unique properties with novel compositions as well as shape, size and interface control.[5] Especially, the fabrication of metal-oxide hollow NSs with controllable shape, size, composition and structural features have been studied and researched because the hollow NSs great promise in versatile applications such as drug delivery, lithium-ion batteries, photocatalysts, gas sensors and dye sensitized solar cells.[6-10] Most of the metal-oxide semiconductor hollow NSs were prepared using template-based fabrication methods.[11-13] Especially, fabrication using carbon spheres as the templates offer more advantages when compared with other templates. Carbon spheres that could be controlled by size and surface properties are porous and hydrophilic, so that the inorganic metal-oxide precursors can be attached easily to the modified surface of the carbon spheres.[14-16]

Zinc gallate ($ZnGa_2O_4$), which has a ternary spinel structure with wide band-gap approximately 4.4 ~ 4.7 eV semiconductor, excellent chemical and thermal stability, cathodoluminescence characteristics at low voltage has shown potential applications in field emission displays, transparent conductors, light emitting diodes and photo-catalysts.[17-19] $ZnGa_2O_4$ is a promising excellent host materials for multicolor-emitting phosphors with doping several activators such as Cr^{3+} and Mn^{2+}, and a self-activated blue emission around 430 nm under excitation with ultraviolet light, especially.[20,21] The thin film and nanocrystalline $ZnGa_2O_4$ have been synthesized by various methods such as a solid-state reaction, sol-gel, hydrothermal and thermal treatments involving vapor-liquid-solid mechanisms.[22-24] Recently, ZnO and Ga_2O_3 nanowires were used as hard templates to fabricate a $ZnGa_2O_4$ nanotubes, in which synthesized ZnO@Ga_2O_3 core-shell nanowires were followed by solid state reaction at high temperatures.[25]

Highly uniform and perfect crystallized $ZnGa_2O_4$ hollow NSs with spinel structure were successfully fabricated by two steps hydrothermal, in which synthesized carbon@$Ga(OH)CO_3$@$Zn(OH)_2$ core-shell-shell NSs with carbon spheres as the templates and then calcined process. We report first the synthesis and characterization of $ZnGa_2O_4$ hollow NSs under controlled several experiment condition.

These hollow NSs could potentially be used in the fabrication of nanoscale functional devices.

Experimental

Synthesis of carbon nanoshperes. Briefly, glucose (10 g) was dissolved in 40 mL of distilled water to form a clear solution. The solution was then sealed in a 50 mL Teflon-lined stainless steel autoclave and maintained at 170 °C for 6 h.

Synthesis of carbon@$Ga(OH)CO_3$@$Zn(OH)_2$ core-shell-shell NSs and $ZnGa_2O_4$ hollow NSs. The carbon@$Ga(OH)CO_3$ core-shell NSs were first prepared by a hydrothermal method using $Ga(NO_3)_3$•xH_2O (99.9%, Sigma-Aldrich) and urea as the raw materials. The as-prepared carbon spheres (150 mg) were added and were well dispersed into a mixed solvent of 48 mL of ethanol and 8 mL of water solution with the assistance of sonication for 30 min. 3 mmol (1.3544 g) of $Ga(NO_3)_3$•xH_2O and 30 mmol (1.8 g) of urea were then dissolved in the carbon colloid solution. Finally, the mixture was transferred to a 100 ml three necked round flask and maintained at 60 °C for 48 hrs with vigorous stirring. After hydrothermal reaction, the products were washed with distilled water and ethanol three times. The washed precipitates were dried by freeze drier at -110 °C. As prepared carbon@$Ga(OH)CO_3$ core-shell NSs were dispersed in a 50 mL solution of zinc acetate dehydrate (ZnAc: 2, 2.5, 3, 3.5 mmol), and then ultrasonicated for 1 min. Finally, the mixture was kept at 60 °C for 12 hrs. After hydrothermal reaction, the products were washed with distilled water and ethanol three times. The final $ZnGa_2O_4$ hollow NSs were obtained after calcination in air at 500 °C for 1 h with a heating rate of 1 °C/min and then firing at 600 ~ 1000 °C for 1 h with a heating rate of 10 °C/min. At elevated firing temperatures, the carbon templates will be completely removed and the required uniform $ZnGa_2O_4$ hollow NSs are obtained.

Materials characterization. The surface morphology of the $ZnGa_2O_4$ hollow NSs as a function of ZnAc ratios and calcination temperatures were observed by using a field-emission scanning electron microscopy (FESEM, JEOL 7500F). High-resolution transmission electron microscopy (HRTEM) and the energy dispersive spectroscopy (EDS) mapping was carried out using a JEM2100F with an accelerating voltage of 200 kV. The crystallinity and structure of the hollow NSs were examined by powder X-ray diffraction (PDR-XRD, Bruker D8 FOCUS) using Cukα radiation. Fourier transform infrared (FTIR, Bruker IFS-66/S) spectroscopy and x-ray photoelectron spectroscopy (XPS) were employed to analyze the chemical bonding within the materials. The thermogravimetry-differential thermal analysis (TG-DTA, Seiko Exstar) was measured in air at a heating rate of 5 °C/min from 30 to 1000 °C to confirm the reaction of carbon spheres and crystallization of $ZnGa_2O_4$ hollow NSs. The optical properties of the $ZnGa_2O_4$ hollow NSs were analyzed using a room temperature cathodoluminescence (MONO CL3+, GATAN) equipped with excitation energy of 10 keV.

Results and discussion

The strategy used to obtain $ZnGa_2O_4$ hollow NSs can be divided into four steps in Fig. 1: 1) synthesis of carbon nanospheres template around 200 nm by hydrothermal approach as reported previously; 2) and 3) formation of core-shell-shell NSs by coating the templates with Ga and Zn precursors; 4) calcination of core-shell-shell NSs in air to remove the carbon cores and make the shell-shell decompose and crystallize completely, which resulting in $ZnGa_2O_4$ hollow NSs.

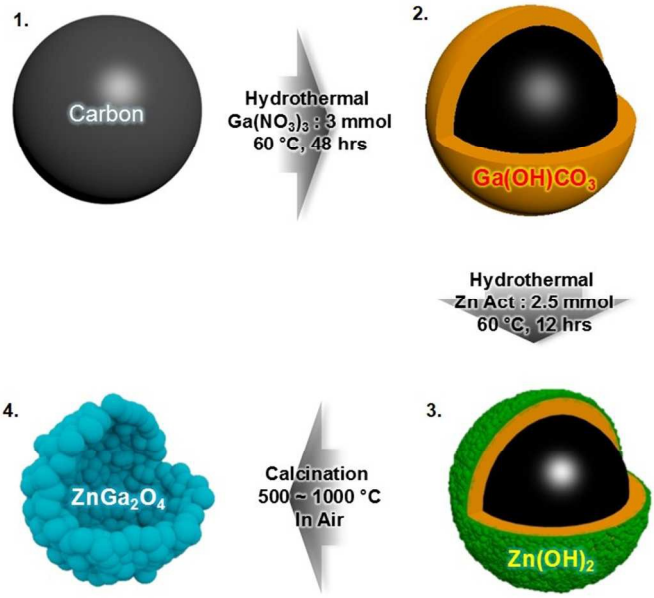

Fig. 1 Illustration of the demonstration and morphology evolution for the $ZnGa_2O_4$ hollow NSs.

Fig. 2(a) and 2(f) show the TEM, HRTEM and EDS mapping images of the prepared core-shell-shell NSs before calcination. The carbon@$Ga(OH)CO_3$@$Zn(OH)_2$ core-shell-shell NSs with 2.5 mmol of ZnAc maintain their spherical shape and are relatively uniform and appear to be well dispersed. The TEM and HRTEM images of the core-shell-shell NSs indicate that the core-shell NSs retained the original uniform shape with diameters of about 200 nm and with a shell thickness of about 15 nm. The carbon@$Ga(OH)CO_3$ core-shell NSs were covered by uniform shell of $Zn(OH)_2$ nanoparticles. In addition, the EDS mapping result shows the relative locations of C, O, Ga and Zn within the core-shell-shell NSs. The Ga and Zn atoms appear in the same position with similar diameters, demonstrating that the Ga atoms were coated as a very thin layer on the surface of the carbon nanospheres and the surface of carbon@$Ga(OH)CO_3$ core-shell NSs was fully occupied by $Zn(OH)_2$ nanoparticles. Moreover, as increasing ZnAc ratios, the $Zn(OH)_2$ nanosheets surround the carbon@$Ga(OH)CO_3$ core-shell NSs (Table S1 and Fig. S1 of ESI†). The composition of carbon@$Ga(OH)CO_3$@$Zn(OH)_2$ core-shell-shell NSs with various ZnAc ratios was assessed by FTIR (Fig. S2 of ESI†).

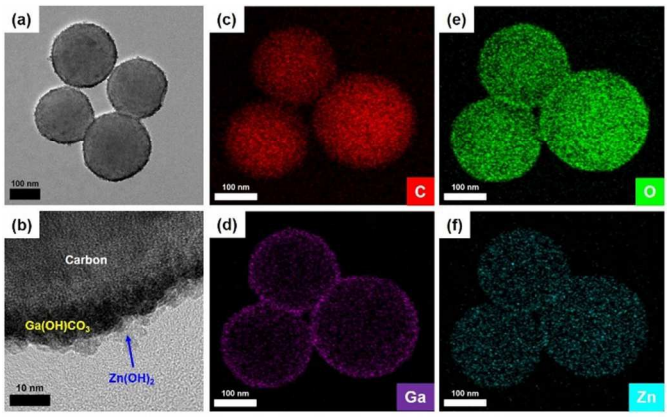

Fig. 2 TEM (a) and HRTEM (b) images of the carbon@$Ga(OH)CO_3$@$Zn(OH)_2$ core-shell-shell NSs at 2.5 mmol of ZnAc before calcination. The element maps showing the spatial distribution of C (c), Ga (d), O (e), and Zn (f) in the carbon@$Ga(OH)CO_3$@$Zn(OH)_2$ core-shell-shell NSs.

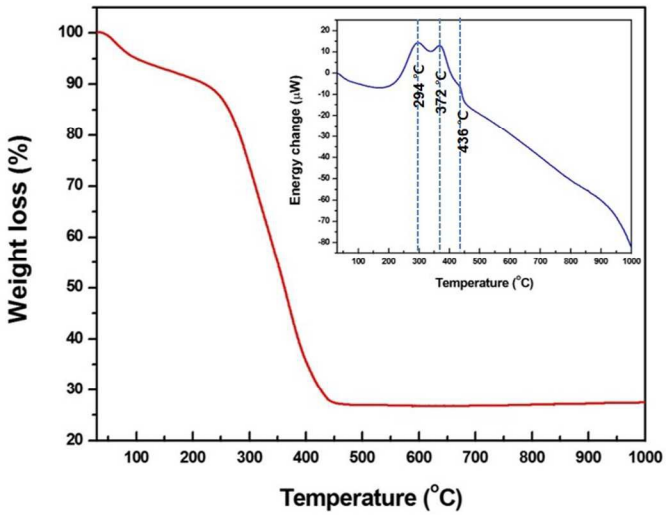

Fig. 3 TG-DTA curves of carbon@$Ga(OH)CO_3$@$Zn(OH)_2$ core-shell-shell NSs at 2.5 mmol of ZnAc.

The TG-DTA curve shows the carbon@$Ga(OH)CO_3$@$Zn(OH)_2$ core-shell-shell NSs before calcination. The TG reveals that during heating in air atmosphere, the weight loss occurs in two steps: One is a slow loss of weight due to the dehydration and densification of carbon nanospheres.[26] The other sharp loss of weight attributed to the burning of the carbon spheres.[27] Also, the residual weight percentage of the carbon@$Ga(OH)CO_3$@$Zn(OH)_2$ core-shell-shell NSs is 27 %, which accounts for the $ZnGa_2O_4$ hollow NSs. The inset in Fig. 3 shows the corresponding DTA results of the samples. DTA curve showed the multiple exothermic peaks of carbon@$Ga(OH)CO_3$@$Zn(OH)_2$ core-shell-shell NSs at 294 and 372 °C and the broad exothermic peaks at 436 °C. The peak intensities of these exothermic peaks suggest further dehydration and densification of carbon nanospheres, the burning of the carbon spheres, and crystallization of $ZnGa_2O_4$. The obtained result of the DTA analysis agree well with the TG analysis.

The PDR-XRD patterns in Fig. 4(a) reveal that the $ZnGa_2O_4$ hollow NSs as function of ZnAc from 2 to 3.5 mmol at 900 °C for 1 h. The cubic $ZnGa_2O_4$ phase is formed in all of the hollow NSs with various ZnAc ratios after calcination, which indicates the successful reaction of the core and shell along the radial direction.[28] The diffraction patterns of spinel $ZnGa_2O_4$ appear at 2.5 mmol of ZnAc, indicating the successful formation of the perfect crystallized $ZnGa_2O_4$ after calcination of the carbon@$Ga(OH)CO_3$@$Zn(OH)_2$ core-shell-shell NSs. However, the Ga_2O_3 and/or ZnO phase still remained in the hollow NSs in the three cases (2, 3 and 3.5 mmol added). The β-Ga_2O_3 diffraction peaks appear in the PDR-XRD pattern of those with original 2 mmol of ZnAc ratio. It suggests that the 2 mmol of ZnAc are too small amount of Zn ions to form uniform $ZnGa_2O_4$ hollow NSs, resulting in remaining the Ga_2O_3 within the annealed hollow NSs. On the contrary, the diffraction patterns at 3.5 mmol show the ZnO and $ZnGa_2O_4$ coexisting in the hollow NSs, suggesting their $Zn(OH)_2$ nanosheets covered carbon@$Ga(OH)CO_3$ core-shell NSs and too amount to obtain single-phase $ZnGa_2O_4$. Fig. 4(b) shows the PDR-XRD patterns of $ZnGa_2O_4$ (ZnAc: 2.5 mmol) hollow NSs with various calcination temperatures for 1 h. All the PDR-XRD patterns were easily indexed to the normal spinel $ZnGa_2O_4$ (JCPDS Card 38-1240). Various diffraction peaks for $ZnGa_2O_4$ were observed for the samples, including those for the (111), (220), (311), (222), (400), (422), (511) and (440) planes. However, the diffraction peaks of β-Ga_2O_3 structure are presented with 1000 °C calcination process, due to the vaporization of Zn ions from $ZnGa_2O_4$ hollow NSs.[29,30] The full width at half maximum (FWHM) of the PDR-XRD peaks for the $ZnGa_2O_4$ hollow NSs decreased with increasing firing temperature from 800 to 1000 °C. This result indicates that the carbon@$Ga(OH)CO_3$@$Zn(OH)_2$ core-shell-shell NSs were perfectly crystallized after controlled calcination steps and increasing firing temperatures.[31] In addition, the grain sizes of $ZnGa_2O_4$ hollow NSs were calculated using the Debye–Scherrer formula (1) based on the main diffraction (311) peak based on the XRD patterns.[32]

$$D_{hkl} = (0.9\times\lambda)/B_{hkl}\cdot\cos\theta \quad (1)$$

A calculated grain size is D and λ is the X-ray wavelength (1.54056 Å). 0.9 is a constant for spherical particles, and B is the FWHM for the diffraction angle. The grain sizes of the $ZnGa_2O_4$ hollow NSs were 11, 17 and 26 nm at a firing temperature of 800 ~ 1000 °C, respectively.

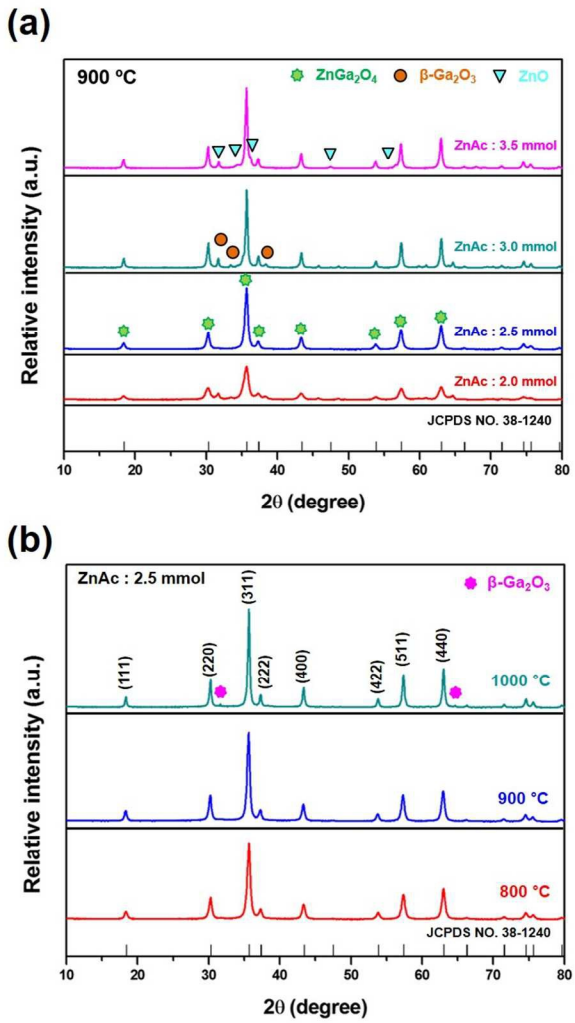

Fig. 4 PDR-XRD (a) and (b) patterns of the calcined $ZnGa_2O_4$ hollow NSs with various ratios of ZnAc from 2 to 3.5 mmol at 900 °C and calcination temperatures from 800 to 1000 °C at 2.5 mmol of ZnAc.

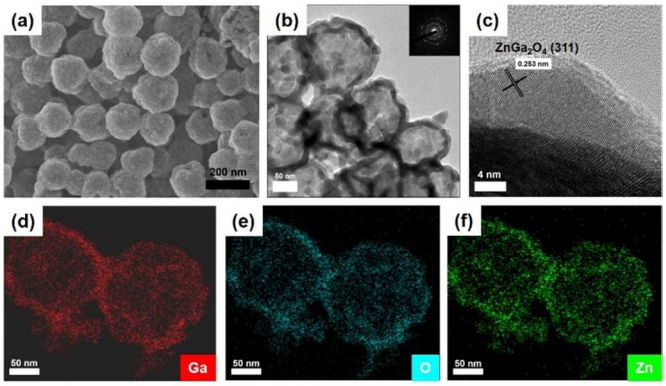

Fig. 5 FESEM (a) and HRTEM (b), (c) images of $ZnGa_2O_4$ hollow NSs. The element maps showing the spatial distribution of Ga (d), O (e), and Zn (f) in the as-prepared $ZnGa_2O_4$ hollow NSs at 2.5 mmol of ZnAc.

Furthermore, the composition of $ZnGa_2O_4$ hollow NSs with various calcination temperature was assessed by FTIR (Fig. S3 of ESI†). Fig. 5(a) ~ (f) show the FESEM and HRTEM images of $ZnGa_2O_4$ (ZnAc: 2.5 mmol) hollow NSs at 900 °C for 1 h. The FESEM image in Fig. 5(a) indicates that the calcined samples consist of uniform hollow NSs with diameters ranging from 100 to 200 nm. The calcined hollow structures were further investigated by TEM. The strong contrast between the dark edge and the pale center is evidence of the hollow structures. The corresponding selective area electron diffraction (SAED) pattern of the $ZnGa_2O_4$ hollow NSs (inset in Fig. 5(b)) clearly shows that the polycrystalline $ZnGa_2O_4$ hollow NSs were obtained. The HRTEM image of the shell is shown in Fig. 5(c). It reveals that the shell is constructed by several the single-crystal nanoparticles and the lattice spacing of around 0.253 nm corresponds to the d spacing of (311) crystal planes of cubic $ZnGa_2O_4$. EDS mapping profile shown in Fig. 5(d) ~ 5(f) obviously indicated that the calcined $ZnGa_2O_4$ hollow NSs contained both gallium and Zinc with homogenous distribution. Also, the purity of the prepared sample at 900 °C has been confirmed by STEM-EDS line analysis (Fig. S4 of ESI†).

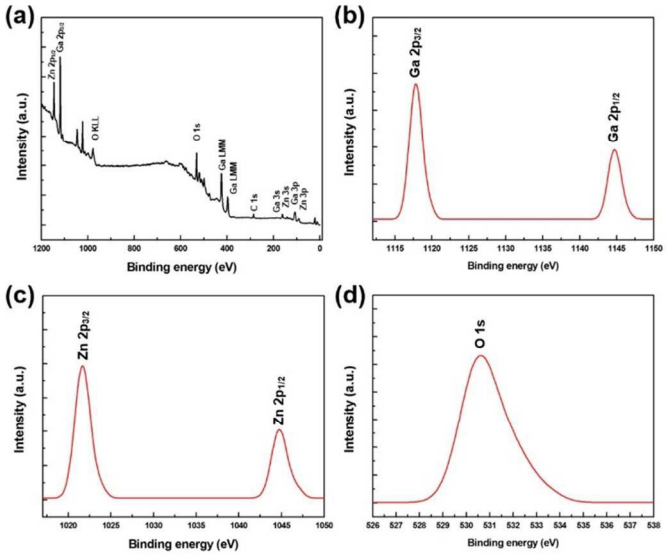

Fig. 6 XPS survey scan (a) of $ZnGa_2O_4$ hollow NSs. XPS spectra of Ga 2p (b), Zn 2p (c) and O 1s (d) of $ZnGa_2O_4$ hollow NSs (ZnAc: 2.5 mmol) at 900 °C for 1 h in Air.

To investigate the composition and surface electron state of $ZnGa_2O_4$ (ZnAc: 2.5 mmol) hollow NSs, we conducted analyses using XPS measurement. Fig. 6(a) ~ (c) show XPS spectra of Zn, Ga and O ions in $ZnGa_2O_4$ hollow NSs, respectively. The fine XPS spectrum reveals Ga $2p_{3/2}$ and Ga $2p_{1/2}$ states at 1117.9 and 1144.8 eV, respectively. The gap between Ga $2p_{3/2}$ and Ga $2p_{1/2}$ is 26.9 eV, which agrees with the reference value of 26.84 eV. For the Zn XPS spectrum shown in Fig. 6(b), the peaks at 1044.8 and 1021.7 eV indicate Zn $2p_{3/2}$ and Zn $2p_{1/2}$ states. The fine XPS spectrum at 530.8 eV correspond to O1s state. Furthermore, the energy separation between Zn $2p_{3/2}$ and Ga $2p_{3/2}$ states (96.2 eV) indicate that as-prepared sample is a complete spinel $ZnGa_2O_4$ without mixture of metal oxide powders such as ZnO and Ga_2O_3.[33,34]

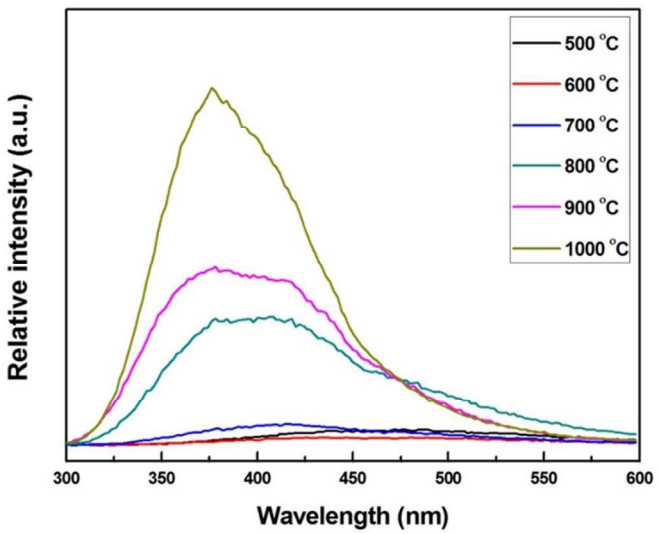

Fig. 7 CL spectra of the $ZnGa_2O_4$ hollow NSs (ZnAc: 2.5 mmol) as a function of the calcination temperatures ranging from 500 to 1000 °C for 1 h in Air.

Fig. 7 show the Cathodoluminescence (CL) spectra of $ZnGa_2O_4$ (ZnAc: 2.5 mmol) hollow NSs as a function of the annealing temperatures from 500 to 1000 °C for 1 h. The optical properties of $ZnGa_2O_4$ NSs such as nanoparticles and wires were strongly dependent on experiment conditions, such as starting materials, reaction atmosphere and the methods utilized. A number of research group reported that emission spectra of $ZnGa_2O_4$ NSs were observed at 360 ~ 550 nm by PL and CL measurements.[35-37] Although the single-phase $ZnGa_2O_4$ hollow NSs are formed via calcination of carbon@$Ga(OH)CO_3$@$Zn(OH)_2$ core-shell-shell NSs in an air environment. The appearance of the emission peak at 376 nm in the CL spectra can be suggested the existence of the oxygen vacancies within the $ZnGa_2O_4$ hollow NSs above calcination temperature 800 °C.[38] A broad blue emission centered at 418 nm was observed, which the emission was mainly attributed to the self-activation center octahedral sites Ga-O group in the spinel structures.[39] In addition, as the calcination temperature increased, UV emission at 376 nm was suddenly increased and emission spectra was blue-shifted. This was attributed to the fact that high calcination temperature at 1000 °C can cause more generated oxygen vacancies in $ZnGa_2O_4$ hollow NSs, due to the evaporation of ZnO. Furthermore, the occupied oxygen vacancies in octahedral sites can cause increase binding energy between Ga and O, which the bond length of the Ga-O was shortened. The blue-shifted emission is attributed to the distorted symmetry of octahedral sites.[40,41]

Conclusion

In summary, using a simple two steps coating and calcination process, we have demonstrated the synthesis of the single-phase $ZnGa_2O_4$ hollow NSs with various ZnAc ratios and calcination temperatures. The perfect crystallized of the $ZnGa_2O_4$ hollow NSs were obtained the carbon@$Ga(OH)CO_3$@$Zn(OH)_2$ core-shell-shell NSs at 2.5 mmol of ZnAc and calcination temperature at 900 °C for 1 h. The formation of uniform polycrystalline $ZnGa_2O_4$ hollow NSs with diameters of around 200 nm and thickness of about 10 ~ 20 nm at 900 °C for 1 h were confirmed by FESEM and HRTEM analysis. The UV and blue emission of $ZnGa_2O_4$ hollow NSs were found to charge transfer Ga^{3+} and O^{2-} ions in octahedral site of spinel structure and distorted symmetry by oxygen vacancies, respectively. Further works are being carried out to explore the potential application of these hollow NSs as photo-catalysts and sensors. Moreover, the core-shell-shell NSs introduced in this letter may be applied to fabricate many other binary metal oxides NSs.

Acknowledgements

This research was supported by Basic Science Research Program through the National Research Foundation of Korea (NRF) funded by the Ministry of Education, Science and Technology (NRF- 2013R1A2A2A01010027).

Notes and references

[a] School of Advanced Materials Science & Engineering, Sungkyunkwan University, Suwon 440-746, Republic of Korea
[b] SKKU Advanced Institute of Nanotechnology (SAINT), Sungkyunkwan University, Suwon 440-746, Republic of Korea
[c] Hyosung Corporation, R&D Business Labs, Anyang 431-080, Republic of Korea

† Electronic Supplementary Information (ESI) available: Tables summarizing experimental details for sample preparation, FESEM images and FTIR data of the carbon@$Ga(OH)CO_3$@$Zn(OH)_2$ core-shell-shell NSs, FTIR, STEM, EDS line scan, CL data and representative band-structure scheme for the UV and blue luminescence in $ZnGa_2O_4$ hollow NSs. See DOI: 10.1039/c000000x/

1 P. Ramasamy, D. H. Lim, J. Kim and J. Kim, *RSC Adv.*, 2014, **4**, 2858.
2 Y. Li, X. Zhao and W. Fan, *J. Phys. Chem. C,* 2011, **115**, 3552.
3 Z. Xue, W. Zhang, X. Yin, Y. Cheng, L. Wang and B. Liu, *RSC Adv.*, 2012, **2**, 7074.
4 B. Koo, H. Xiong, M. D. Slater, V. B. Prakapenka, M. Balasubramanian, P. Podsiadlo, C. S. Johnson, T. Rajh and E. V. Shevchenko, *Nano Lett.*, 2012, **12**, 2429.
5 Q. Yuan, H.-H. Duan, L.-L. Li, L.-D. Sun, Y.-W. Zhang, C.-H. Yan, *J. Colloid Interf. Sci.*, **2009**, 335, 151.
6 W. Xiao, W.-H. Chen, J. Zhang, C. Li, R.-X. Zhuo and X.-Z. Zhang, *J. Phys. Chem. B*, 2011, **115**, 13796.
7 W. Wang, Y. Xiao, X. Zhao, B. Liu and M. Cao, *CrystEngComm*, 2014, **16**, 922.
8 Y. Zeng, X. Wang, H. Wang, Y. Dong, Y. Ma and J. Yao, *Chem. Commun.*, 2010, **46**, 4312.
9 X. Lai, J. Li, B. A. Korgel, Z. Dong, Z. Li, F. Su, J. Du and D. Wang, *Angew. Chem. Int. Ed.*, 2011, **50**, 2738.
10 X. Wu, G. Q. (Max) Lu and L. Wang, *Energy Environ. Sci.*, 2011, **4**, 3565.
11 J. Xu, L. Li, F. He, R. Lv, P. Yang, *Electrochimica Acta*, 2014, **148**, 211.
12 Y. Wang, P. Gao, D. Bao, L. Wang, Y. Chen, X. Zhou, P. Yang, S. Sun and M. Zhang, *Inorg. Chem.*, 2014, **53**, 12289.
13 D. Bao, P. Gao, L. Wang, Y. Wang, Y. Chen, G. Chen, G. Li, C. Chang and W. Qin, *ChemPlusChem*, 2013, **78**, 1266.
14 M.-M. Titirici, M. Antonietti and A. Thomas, *Chem. Mater.*, 2006, **18**, 3808.
15 C.-A. Wang, S. Lia and L. An, *Chem. Commun.*, 2013, **49**, 7427.
16 X. Guo, X. Liu, B. Xu, T. Dou, *Colloid Surface A*, 2009, **345**, 141.

17 V. R. Kumar, K. V. Narasimhulu, N. O. Gopal, H.-K. Jung, R. P. S. Chakradhar, J. L. Rao, *J. Phys. Chem. Solids*, 2004, **65**, 1367.
18 L.-C. Tien, C.-C. Tseng, Y.-L. Chen, C.-H. Ho, *J. Alloy Compd.*, 2013, **555**, 325.
19 M.-Y. Lu, X. Zhou, C.-Y. Chiu, S. Crawford and S. Gradečak, *ACS Appl. Mater. Interfaces*, 2014, **6**, 882.
20 Y. Zhuang, J. Ueda and S. Tanabe, *Appl. Phys. Express*, 2013, **6**, 052602.
21 N. F. Santos, A. J. S. Fernandes, L. C. Alves, N. A. Sobolev, E. Alves, K. Lorenz, F. M. Costa, T. Monteiro, *Nucl. Instrum. Meth. B*, 2013, **306**, 195.
22 Q. Liu, D. Wu, Y. Zhou, H. Su, R. Wang, C. Zhang, S. Yan, M. Xiao and Z. Zou, *ACS Appl. Mater. Interfaces*, 2014, **6**, 2356.
23 M. Lei, Q.R. Hu, X. Wang, S.L. Wang, W.H. Tang, *J. Alloy Compd.,* 2010, **489**, 663.
24 M. M. Can, G. H. Jaffari, S. Aksoy, S. I. Shah, T. Fırat, *J. Alloy Compd.*, 2013, **549**, 303.
25 U. K. Gautam, Y. Bando, J. Zhan, P. M. F. J. Costa, X. Fang and D. Golberg, *Adv. Mater.*, 2008, **20**, 810.
26 X. Sun and Y. Li, *Angew. Chem. Int. Ed.*, 2004, **43**, 3827.
27 G. Jia, M. Yang, Y. Song, H. You and H. Zhang, *Cryst. Growth Des*., 2009, **9**, 301.
28 K.-W. Chang and J.-J. Wu, *J. Phys. Chem. B*, 2005, **109**, 13572.
29 Y. E. Lee, D. P. Norton and J. D. Budai, *Appl. Phys. Lett.*, 1999, **74**, 3155.
30 A. C. Tas, P. J. Majewski and F. Aldinger, *J. Mater. Res.*, 2002, **17**, 1425.
31 M. Shang, W. Wang and H. Xu, *Cryst. Growth. Des.*, 2009, **9**, 991.
32 M. Gopalakrishnan, V. Purushothaman, V. Ramakrishnan, G. M. Bhalerao and K. Jeganathan, *CrystEngComm*, 2014, **16**, 3584.
33 A. R. Phani, S. Santucci, S. Di Nardo, L. Lozzi, M. Passacantando, P. Picozzi, C. Cantalini, *J. Mater. Sci*., 1998, **33**, 3969.
34 L. Zou, X. Xiang, M. Wei, F. Li and D. G. Evans, *Inorg. Chem.,* 2008, **47**, 1361.
35 P. M. Aneesh, K. M. Krishna and M. K. Jayaraj, *J. Electrochem. Soc.*, 2009, **156**, K33.
36 L. Xu, Y. Su, Q. Zhou, S. Li, Y. Chen and Y. Feng, *Cryst. Growth Des.,* 2007, **7**, 810.
37 B. Liu, Y. Bando, B. Dierre, T. Sekiguchi, C. Tang, M. Mitome, A. Wu, X. Jiang and D. Golberg, *Nanotechnology*, 2009, **20**, 365705.
38 Y. J. Li, M. Y. Lu, C. W. Wang, K. M. Li and L. J. Chen, *Appl. Phys. Lett.*, 2006, **88**, 143102.
39 H.-J. Byun, J.-U. Kim and H. Yang, *Nanotechnology,* 2009, **20**, 495602.
40 Y. Yuan, W. Du and X. Qian, *J. Mater. Chem.*, 2012, **22**, 653.
41 J. S. Kim, H. I. Kang, W. N. Kim, J. I. Kim, J. C. Choi, H. L. Park, G. C. Kim, T. W. Kim, Y. H. Hwang, S. I. Mho, M.-C. Jung and M. Han, *Appl. Phys. Lett.*, 2003, **82**, 2029.

Graphical Abstract

Highly uniform and perfect crystallized $ZnGa_2O_4$ hollow NSs successfully fabricated via carbon@$Ga(OH)CO_3$@$Zn(OH)_2$ core-shell-shell nanostructures by two steps hydrothermal method.